Functional Characterization of JMJD2A, a Histone Deacetylase- and Retinoblastoma-binding Protein

THE JOURNAL OF BIOLOGICAL CHEMISTRY
Vol. 280, No. 31, Issue of August 5, pp. 28507–28518, 2005

Printed in U.S.A.

Functional Characterization of JMJD2A, a Histone Deacetylase- and Retinoblastoma-binding Protein*[S]

Received for publication, December 6, 2004, and in revised form, May 26, 2005
Published, JBC Papers in Press, May 31, 2005, DOI 10.1074/jbc.M413687200

Steven G. Gray,[a,b,c,d,e] Antonio H. Iglesias,[a,e] Fernando Lizcano,[a,e,f] Raul Villanueva,[a] Sandra Camelo,[a] Hisaka Jingu,[g] Bin T. Teh,[c] Noriyuki Koibuchi,[g] William W. Chin,[h] Efi Kokkotou,[i] and Fernando Dangond[a,j]

From the [a]Laboratory of Transcriptional and Immune Regulation, Brigham and Women's Hospital Laboratories, Cambridge, Massachusetts 02139, the [b]Receptor Biology Laboratory, Hagedorn Research Institute, Novo Nordisk, Niels Steensens Vej, Gentofte DK-2820, Denmark, the [c]Laboratory of Cancer Genetics, Van Andel Research Institute, Grand Rapids, Michigan 49503, the [d]Thoracic Oncology Research Group, Departments of Oncology and Clinical Medicine, Institute of Molecular Medicine, Trinity Sciences Health Center, St. James's Hospital, Dublin 8, Ireland, the [f]Laboratory of Molecular Biology, School of Medicine, La Sabana University, Bogota, Colombia, the [g]Department of Physiology, Gunma University School of Medicine, Maebashi, Gunma 371-8511, Japan, [h]Gene Regulation Research, Eli Lilly Co., Indianapolis, Indiana 46285, the [i]Molecular Medicine Laboratory and Macromolecular Crystallography Unit, Division of Experimental Medicine, Department of Medicine, Beth Israel Deaconess Medical Center, Harvard Medical School, Boston, Massachusetts 02115

To effectively direct targeted repression, the class I histone deacetylases (HDACs) associate with many important regulatory proteins. In this paper we describe the molecular characterization of a member of the Jumonji domain 2 (JMJD2) family of proteins, and demonstrate its binding to both class I HDACs and the retinoblastoma protein (pRb). JMJD2 proteins are characterized by the presence of two leukemia-associated protein/plant homeodomain (LAP/PHD) zinc fingers, one JmjN, one JmjC (containing an internal retinoblastoma-binding protein 2 (RBBP2)-like sequence), and two Tudor domains. The first member of this group, JMJD2A, is widely expressed in human tissues and cell lines, and high endogenous expression of JMJD2A mRNA was found in several cell types, including human T-cell lymphotropic virus 1 (HTLV-1)-infected cell lines. JMJD2A and JMJD2B exhibit cell type-specific responses to the HDAC inhibitor trichostatin A. We show that the JMJD2A protein associates *in vivo* with pRb and class I HDACs, and mediates repression of E2F-regulated promoters. In HTLV-1 virus-infected cells, we find that JMJD2A binds to the viral Tax protein. Antibodies to JMJD2A recognize the native protein but also a half-sized protein fragment, the latter up-regulated in THP-1 cells during the G_2/M phase of the cell cycle. The ability of JMJD2A to associate with pRb and HDACs and potentiate pRb-mediated repression of E2F-regulated promoters implies an important role for this protein in cell proliferation and oncogenesis.

The tight confines of chromatin have necessitated the evolution of specialized chromatin remodeling complexes to achieve appropriate regulation of gene expression within the mammalian cell. One such mechanism that has recently been elucidated involves the acetylation of the histone tails within the nucleosome. The histone deacetylase (HDAC)[1] family of proteins is involved with removing such modifications, and its members have been subgrouped into three classes depending upon their similarity to yeast proteins (1, 2). Since the isolation of the first HDAC many members of this family have been identified, currently consisting of at least 18 members (1–3). Critical roles for these proteins have been identified in many aspects of cell function.

The product of the retinoblastoma gene, pRb, has been shown to have multiple roles in cellular processes, including regulation of apoptosis and the cell cycle (4). pRb interacts with E2F family transcription factors and blocks their activity during the G_0 and G_1 phases of the cell cycle. E2F proteins activate the expression of many genes involved in cell cycle progression, including cyclins A and E, as well as other proteins and enzymes required for DNA replication (5). Binding sites for E2F are found in the promoters of genes whose expression occurs at the G_1/S transition, and repression of the promoters containing E2F-binding sites has been shown to involve binding of E2F/pRb pocket protein complexes to these sites.

Previous studies have identified two distinct, although not mutually exclusive, mechanisms for the transcription repression function of pRb (5–7). The first mechanism involves the direct interaction of pRb with the E2F transactivation domain, resulting in masking of this domain and blocking its ability to stimulate transcription (8). The second mechanism is based on the ability of pRb to recruit chromatin remodeling proteins, such as HDACs, and assemble transcription repression complexes at E2F-regulated promoters (9–12). A separate series of experiments demonstrated that RBBP1, a known pRb interacting protein, acts as a bridge to recruit HDACs 1–3 to pRb-E2F complexes (13, 14).

The JMJD2 family of proteins has recently been identified *in*

* This work was supported in part by a grant from the Van Andel Research Institute (to B. T. T.) and National Institutes of Health Grant CA80084 (to F. D.). The costs of publication of this article were defrayed in part by the payment of page charges. This article must therefore be hereby marked "*advertisement*" in accordance with 18 U.S.C. Section 1734 solely to indicate this fact.

[S] The on-line version of this article (available at http://www.jbc.org) contains Fig. S1 and data.

[e] These authors contributed equally to this work.
[j] To whom correspondence should be addressed: Laboratory of Transcriptional and Immune Regulation, Brigham and Women's Hospital Laboratories, 3rd floor, 65 Landsdowne St., Cambridge, MA 02139. Tel.: 617-768-8597; Fax: 617-768-8595; E-mail: fdangond@rics.bwh.harvard.edu.

[1] The abbreviations used are: HDAC, histone deacetylase; pRb, retinoblastoma protein; LAP, leukemia-associated protein; PHD, plant homeodomain; aa, amino acid(s); GST, glutathione *S*-transferase; CMV, cytomegalovirus; EYFP, enhanced yellow fluorescent protein; HA, hemagglutinin; RT, reverse transcriptase; RPA, RNase protection assay; AD, activation domain; TK, thymidine kinase; TSA, trichostatin A; HTLV-1, human T-cell lymphotropic virus 1; RBBP, retinoblastoma-binding protein.

silico (15). Here we describe the molecular characterization of JMJD2A, a nuclear and cytoplasmic member of this family that participates as a pRb-HDAC complex component. JMJD2A contains two LAP/PHD (leukemia-associated protein/plant homeodomain) zinc fingers, one JmjN, one JmjC (containing an internal RBBP2-like sequence), and two Tudor domains, and promotes histone deacetylation and gene repression *in vivo*, through its association with HDACs and pRb. Multiple truncated fragments of JMJD2A bind pRb, suggesting that the pRb A/B pocket is not the only interaction site. JMJD2A also binds the viral protein Tax in HTLV-1-infected cells. The property of JMJD2A to both associate with pRb/HDACs and Tax and to mediate transcriptional repression suggests an important role for this protein in cell proliferation and transformation, and provides new insights into the molecular mechanisms of pRb function.

MATERIALS AND METHODS

Library Screening and Plasmid Construction—A human fetal liver λgt11 cDNA library (Clontech number HL1064b) was screened under low stringency conditions, using as a probe a DNA fragment corresponding to the DNA-binding domain of human Sp1, as described previously (16). The full-length KIAA0677 cDNA was a gift from T. Nagase (Kazusa DNA Research Institute). The region of JMJD2A (aa 661–1064) originally identified in the Sp1 screen was cloned directly into $pFGAL_{94}XR$ (17), for use in repression assay and chromatin immunoprecipitation experiments. The dihydrofolate reductase (DHFR) promoter-Luc construct containing three E2F-binding sites, pSG5-HA-pRb, pSG5-HA-pRbΔ22, and GAL4-pRb (18), were gifts from W. Kaelin (Dana-Farber Cancer Institute). A full-length FLAG-tagged cDNA for human HDAC3 was obtained from E. Seto (Moffitt Cancer Center) (19).

A full-length fusion of JMJD2A to EYFP was generated by PCR of the full-length JMJD2A cDNA with primers incorporating appropriate restriction enzyme sites: EYFP-N1 JMJD2A FWD (HindIII), 5′-CGAAGCTTATGGCTTCTGAGTCTGAAACTCTGAATCCC-3′; EYFP-N1 JMJD2A REV (SalI), 5′-GGATGTCGACTTCTCCATGATGGCCCGGTATAGTGC-3′. The PCR products were first cloned into pCR II (Invitrogen), from which JMJD2A was isolated using HindIII/SalI and cloned into similarly digested EYFP-N1 (Clontech). The construct was sequenced to verify that the fusion was in-frame.

Bioinformatic and Phylogenetic Analysis—The accession numbers for the protein sequences used for alignments are as follows: hJMJD2A (NP_055478), hJMJD2B (NP_055830), hJMJD2C/hGASC1 (NP_055876), hJMJD2D (XP_061849), hJMJD2E (AP002383.3), hJMJD2F (AP001264.4), mJMJD2A (AAH28866), mJMJD2B (AAH07145), mJMJD2C/mGASC1 (NP_659036), mJMJD2D (XP_143503), rJMJD2A (XP_233441), rJMJD2D (XP_235826), cJMJD2A (XP_422410), cJMJD2B (XP_425914), cJMJD2C (XP_424815), xtJMJD2A (C_scaffold_25000012), fJMJD2A (FRUP00000161146), fJMJD2C (FRUP00000151439), tnJMJD2.1 (CAF92874), tnJMJD2.2 (CAF91827), tnJMJD2.3 (CAG01941), zJMJD2A (AAH47193), dJMJD2s (AAF59172 and AAF58413), agJMJDs (XP_309467 and XP_308975), amJMJD2 (XP_395616), crJMJD2 (C_50086) and ceJMJD2D (CAB54451), where h stands for *Homo sapiens*, m for the mouse *Mus musculus*, r for the rat *Rattus norvegicus*, c for the chicken *Gallus gallus*, xt for the frog *Xenopus tropicalis*, f for the pufferfish *Fugu rubripes*, tn for the pufferfish *Tetraodon nigroviridis*, z for the zebrafish *Danio rerio*, d for *Drosophila melanogaster*, ag for the mosquito *Anopheles gambiae*, am for the honeybee *Apis mellifera*, cr for *Clamydomonas reinhardtii*, and ce for *Caenorhabditis elegans*.

Protein sequences were obtained from the following public data bases: NCBI (www.ncbi.nlm.nih.gov), the UCSC Genome Browser (genome.ucsc.edu), the FUGU Rubripes genome data base version 3.0 (genome.jgi-psf.org/fugu), *Xenopus tropicalis* genome data base assembly version 2.0 (genome.jgi-psf.org/xenopus), and the *Chlamydomonas* genome assembly version 2.0 (genome.jgi-psf.org/chlamy). Protein sequence alignments were generated using ClustalW (searchlauncher.bcm.tmc.edu/multi-align/multi-align.html), and the conserved residues obtained from this analysis were highlighted using BOXSHADE (www.ch.embnet.org/software/Box_form.html). Phylogenetic analysis was carried out using the MEGA 3 software package (www.megasoftware.net) (20). Structurally conserved elements were identified using SMART (smart.embl.de) (21).

Zinc Binding Assay—GST fusion proteins were expressed in *Escherichia coli* BL21 cells and were purified on glutathione-Sepharose 4B (Amersham Biosciences). Protein samples were analyzed by SDS-PAGE, transferred onto a nitrocellulose filter, denatured with 6 M guanidine hydrochloride for 30 min, followed by three washes in metal binding buffer A (100 mM Tris, 50 mM NaCl, 5 mM dithiothreitol, pH 7.5) for 1 h with three buffer changes. Subsequently, the blot was probed with 50 μCi of $^{65}ZnCl_2$ (PerkinElmer Life Sciences) in 20 ml of buffer A for 1 h, washed three times with buffer A, rinsed with deionized H_2O, and autoradiographed for 16 h at −80 °C with an intensifying screen. After autoradiography, the filter was stained with 0.1% Amido Black (Sigma) in 45% methanol, 10% acetic acid for protein visualization.

Cell Cultures and Treatment—Hep3B, ACHN, HeLa, U2OS, Saos-2, and 293 cell lines were grown in Dulbecco's modified Eagle's medium containing 10% fetal calf serum, 2 mM L-glutamine, and 100 units/100 μg/ml of penicillin/streptomycin. HT1376 bladder carcinoma cells were grown in Dulbecco's modified Eagle's medium supplemented with 10% fetal calf serum, 10 mM Hepes, 2 mM L-glutamine, and 100 units/100 μg/ml of penicillin/streptomycin. Saos-2 cells were supplemented with L-glutamine (BioWhittaker). T-cell clones were stimulated with the polyclonal activator phytohemagglutinin (1 μg/ml) and irradiated feeders for continuous growth. All cells were plated on sterile Petri dishes or 96-well plates and incubated at 37 °C with 6% CO_2 and 96% humidity. Human myeloid leukemia THP-1 cells, Epstein-Barr virus lymphoblasts, HUT102, and C81 cells were grown in complete medium (RPMI media supplemented with 10% fetal calf serum, 10 mM Hepes, 2 mM L-glutamine, and 100 units/100 μg/ml of penicillin/streptomycin). Complete medium plus interleukin-2-containing T-Stim (Collaborative Biomedical Products) was used for T-cell clone cultures. Trichostatin A was purchased from Upstate Biochemicals, dissolved in Me_2SO, and cells were treated as previously described (22).

Transient Transfections—THP-1 cells were transfected by electroporation as reported previously (23), and other cells were transfected with various amounts of effector plasmids, 1.7 μg of luciferase reporter and 1 μg of CMV-β-galactosidase using the calcium phosphate coprecipitation method, as described previously (17). 293 cells used for the mammalian two-hybrid assay were transfected by lipofection with the Lipofectamine Plus kit (Invitrogen). Plasmid pcDNA3 was used as filler DNA to balance the amount of transfected DNA in all experiments. Cells were harvested 48 h post-transfection, and luciferase and β-galactosidase activities were measured in the lysates, as described (17). Transfections performed in triplicate are presented as a mean ± S.E.

For fluorescent protein analysis HEK-293T cells were transfected using FuGENE (Roche) according to the manufacturer's instructions. Plasmid pBluescript II SK(−) (Stratagene) was used as filler DNA. EYFP fluorescence was monitored 48 h post-transfection.

For E2F promoter construct luciferase assay, 293 cells were trypsinized and plated in 24-well plates at a final concentration of 5×10^5 cells per well in 2 ml of medium, 24 h prior to transfection. Using the FuGENE 6 (Roche) transfection reagent, cells were transfected with the following various concentrations of effector plasmids, 1.0 μg of JPTR1, 0.5 μg of pRb, 0.7 μg of dihydrofolate reductase luciferase reporter, and 0.1 μg of pCMV-β-Gal. Cells were harvested 48 h post-transfection, and levels of luciferase and β-galactosidase were measured using the Dual Light System (Applied Biosystem), a chemiluminescent reporter gene assay system for the combined detection of luciferase and β-galactosidase.

Antibody Generation, Immunocytochemistry, and Western Blot Analyses—Rabbit anti-JMJD2A and -JMJD2B were raised using the following synthetic peptides: JMJD2A, TEKEVKQEKKRQ; and JMJD2B, STFSKLKMEIK. Immunocytochemistry with these antibodies was then performed on rat brain tissues (medulla and pons). Adult Sprague-Dawley rats were transcardially perfused with 4% *para*-formaldehyde/phosphate-buffered saline, and the brain dissected out. Fifty-μm thick frozen sections were taken from brains for subsequent immunocytochemical analysis. The procedure for immunocytochemistry has been described elsewhere (24), and immunoreactivity was visualized with 3,3′-diaminobenzidine. For Western blot analysis, cells were harvested, washed, and lysed in extraction buffer (50 mM Tris, 10% glycerol, 150 mM NaCl, pH 8.0) by rocking at 4 °C for 30 min. Following centrifugation, the whole cell extracts were removed and stored at −80 °C prior to use. Proteins were resolved by electrophoresis using precast a 4–20% gradient Tris glycine gel (NOVEX, San Diego, CA), and transferred to a nitrocellulose membrane filter (Millipore, Bedford, MA). The membranes were blocked with 5% nonfat milk and probed with rabbit polyclonal antibodies to JMJD2A at a dilution of 1:1000 for 1 h, then with horseradish peroxidase-conjugated anti-rabbit antibodies (Affinity Bioreagents, Golden, CO) at a dilution of 1:10,000. α-FLAG and α-HA antibodies were also used. The bands were visualized by using the enhanced chemiluminescence system (PerkinElmer Life Sciences) and

exposing to x-ray film (Eastman Kodak).

RNA Isolation and RT-PCR from Multiple Cell Lines—Total RNA was isolated from 5×10^6 cells using the TRIzol method (Invitrogen). RNA was resuspended in diethyl pyrocarbonate (Sigma)-treated water, and its concentration and purity were determined using OD 260/280 (Carey 64 UV Spectrophotometer). RNA (1 μg) was used in a cDNA synthesis reaction using 200 units of Moloney murine leukemia virus-reverse transcriptase (Invitrogen) with Retroscript Kit reagents (Ambion, Austin, TX) for RT-PCR analysis. Following the manufacturer's protocol, RNA was incubated with 5 μl of oligo(dT) primer (Ambion) at 70 °C for 10 min. RNA was transferred to ice, the Superscript II mixture was added, and cDNA synthesis was allowed to occur at 42 °C for 1 h in the presence of ~20 units of RNasin (Promega). Three μl of cDNA were used in 50 μl of PCR using recombinant *Taq* polymerase (Invitrogen) at 0.25 units/sample. One μl of 10 mM dNTP mixture (Invitrogen) per sample was used for each reaction. PCR was performed for *JMJD2A*, *HDAC3*, and *β-actin*. Specific primers were as follows: JMJD2A, forward, 5′-AATCGGATCCATGGCTTCTGAGTCTGAAACTC-3′, reverse, 5′-AGCTGGGCCCGGATCCTCTTGAGTCACCTTGTCAAA-3′; HDAC3, forward, 5′-CGCCGGCACCATGGCCAAGA-3′, reverse, 5′-GCTGGGTTGCTCCTTGCAGA-3′; β-actin, 5′-AACCCCAAGGCCAACCGCGAGAAGATGACC-3′, reverse, 5′-GGTGATGACCTGGCCGTCAGGAGCTCGTA-3′. The JMJD2A primers yield a 790-base product, which spans nucleotides (1–790), and includes the JmjN and most of the JmjC domains. The HDAC3 primers yield a PCR product of 427 bases. The β-actin primers yield a PCR product of 406 bases. PCR conditions were as follows: for *JMJD2A*, denaturing was performed at 94 °C for 1 min, annealing at 62 °C for 1 min, and extension at 72 °C for 2 min; for *HDAC3*, denaturing was done at 94 °C for 1 min, annealing at 68 °C for 1 min, and extension at 72 °C for 2 min; for *β-actin*, denaturing was done at 94 °C for 1 min, annealing at 68 °C for 1 min, and extension at 72 °C for 2 min. Following 35 PCR cycles, all samples were allowed to extend at 72 °C for 10 min. All PCR were performed in a model PTC-100 programmable thermal controller (MJ Research, Inc., Watertown, MA). Twenty μl of each of the PCR products were electrophoresed in 1% agarose (Invitrogen) gels. The gels were then stained with ethidium bromide, placed on a UV transilluminator, and photographed.

Northern Blot Analysis—Human multiple tissue and tumor cell line Northern blots (Clontech numbers 7760-1 and 7757-1, respectively) were probed with a radiolabeled DNA fragment corresponding to *JMJD2A* residues 661–1064, at 42 °C for 16 h. The blots were washed twice with 1× SSC, 0.5% SDS at room temperature for 15 min, followed by 0.5× SSC, 0.5% SDS at 65 °C for 15 min. After autoradiography, the probe was removed, and hybridization was repeated using a *β-actin* probe (Clontech).

RNase Protection Assay (RPA)—T7 and Sp6 RNA polymerases (Invitrogen) were used to make antisense probes from the following templates according to the protocol provided in the RPA II kit (Ambion). When incorporating radioactivity into the probe, radioactive [^{32}P]UTP with a specific activity of 800 Ci/mmol was used. Cold UTP was added such that the final UTP specific activity was 80 Ci/mmol for the *β-actin* probe and 400 Ci/mmol for the others. The *β-actin* probe used in this study is commercially available (Ambion). The probes used to measure *JMJD2A* and *JMJD2B* were prepared as follows. To measure *JMJD2A* expression, a 300-base pair fragment was amplified from full-length *JMJD2A* cDNA (nucleotides 1375–1675) using the amplification conditions as described above and the following primers: JMJD2A RPA forward, 5′-CCACTGAAGTCAAATTTGAAGAGC-3′; JMJD2A RPA reverse, 5′-GCTCTCCCACAGTGACCCTGCC-3′.

The PCR amplification product was isolated from agarose using a Qiaex II Gel extraction kit (Qiagen) and cloned into pCRII using TOPO TA cloning (Invitrogen). The resulting plasmid could be linearized using EcoRV, and an appropriate antisense probe generated using Sp6 RNA polymerase of which 300 bases hybridize specifically to *JMJD2A* RNA. This region spans amino acids 459–558, between the JmJC and PHD domains of JMJD2A.

JMJD2B expression was measured using a 351-bp EcoRI/XbaI fragment of *JMJD2B* cDNA cloned into the same sites of pGem3zf(+) (Promega). This region spans nucleotides 3582–3933 of the full-length JMJD2B mRNA and lies within the 3′-untranslated region. Following linearization with EcoRI, Sp6 RNA polymerase was used to transcribe probe. Both plasmid templates described were sequence verified to confirm the veracity of the cloned insert.

Quantification of the RPA results was obtained using a BAS-100 phosphorimager (Fuji). The levels of *β-actin* mRNA were utilized as the internal control in each case. The values for each experimental gene examined were normalized to the internal control for each sample.

Mammalian Two-hybrid Analysis—-Protein-protein interactions *in vivo* were detected using the mammalian two-hybrid system (Stratagene number 211344) in 293 cells. In this assay, a gene encoding a protein of interest (protein X) was fused to the DNA-binding domain of the yeast protein GAL4, whereas another gene suspected of interacting with protein X (protein Y) was fused to the transcriptional activation domain of the mouse protein NF-κB. If protein X and protein Y interact, they create a functional transcription activator by bringing the activation domain into close proximity with the DNA-binding domain; this can be detected by expression from a luciferase reporter gene under control of a promoter with GAL4-binding sites.

Various *JMJD2A* cDNA fragments were cloned into the pCMV-AD vector (Stratagene), to produce JMJD2A fused to the NF-κB activation domain (AD). These constructs (0.1 μg) were used in calcium phosphate-based cotransfection experiments with the reporter plasmid pFR-Luc (1.7 μg, Stratagene), which contains a synthetic promoter with five GAL4-binding sites upstream of the luciferase gene, along with control activation domain constructs pAD-SV40T and pAD-TRAF, and binding domain constructs pBD-Rb and control pBD-p53 (0.1 μg each; all from Stratagene). Luciferase activity was then measured in cell extracts.

The full-length cDNA and fragments of JPTR1 used in the mammalian two-hybrid experiments described within were derived by PCR, and the primer sets incorporated a BamHI restriction site for cloning purposes and were as follows: full-length (aa 1–1064), forward 5′-AATCGGATCCATGGCTTCTGAGTCTGAAACTC-3′, reverse, 5′-AATCGATCCCTACTCCATGATGGCCCGTTATAG-3′. Fragments Thr-660 (aa 1–660 containing the JmjN and JmjC domains), and Met-867 (aa 1–867 containing the JmjN, JmjC, and PHD domains) used the same forward primer from the full-length oligo pair but had the following reverse primers: 5′-AATCGGATCCGGTCTCATTGAATTCCTTCTCA-3′ (Thr-660) and 5′-AATCGGATCCCATCACACCGGCAGCCTGGGCGCAG-3′ (Met-867). Fragments Met-661 (aa 661–1064 containing the PHD and Tudor domains) and Met-868 (aa 868–1064 containing only the Tudor domains) use the reverse primer from the full-length oligo pair but have the following forward primers: 5′-AATCGGATCCATGGCCCAACAGGCCCCTCA-3′ (Met-661) and 5′-AATCGGATCCATGCAGCCTGACGACTGGCCT-3′ (Met-868). The amino acid prior to the numbers indicate at which each fragment starts and the numbers indicate the position of this amino acid in relation to the full-length protein.

The conditions used to amplify these fragments were as follows: ~100 ng of template (full-length *JMJD2A* cDNA plasmid) was combined with 0.5 μM of each primer in the presence of 1.5 mM $MgCl_2$, 0.2 mM dNTPs, and 1 unit of *Taq* DNA polymerase with the supplied buffer (Invitrogen) in a total volume of 50 μl. Cycling conditions were 95 °C for 5 min followed by 30 cycles of 1 min at 95 °C, 1 min at 55 °C, 2 min at 72 °C with a final extension at 72 °C for 10 min. PCR products were extracted once with phenol-chloroform, precipitated, and then subsequently digested with BamHI. Following digestion the fragments were run into 1% agarose, and the bands were isolated and purified using the Qiaquick gel extraction kit (Qiagen). Following purification the fragments were subsequently ligated into pCMV-AD (Stratagene) for the mammalian two-hybrid assay (used against Rb-GAL4 from W. Kaelin), and transformed into *E. coli*.

Immunoprecipitation—Thirty-six hours post-transfection, HeLa cells were washed with phosphate-buffered saline and harvested in lysis buffer (50 mM Tris-HCl, pH 8.0, 150 mM NaCl, 10% glycerol, 0.5% Triton X-100) containing protease inhibitors. The cells were lysed for 20 min at 4 °C, followed by centrifugation at 14,000 × *g* for 10 min. Proteins were immunoprecipitated from the supernatant by overnight incubation at 4 °C with anti-human pRb G3-245 (BD Pharmingen), anti-His (Invitrogen), anti-HA (Santa Cruz Biotechnology), anti-mSin3 (Santa Cruz Biotechnology), anti-HDAC1 (Affinity Bioreagents), anti-HDAC3 (Affinity Bioreagents), or M2 anti-FLAG antibodies. Immunoprecipitated proteins were recovered on protein A-agarose (Upstate Biotechnology), washed three times for 5 min at room temperature with 50 mM Tris-HCl, pH 8.0, 150 mM NaCl, 1 mM EDTA, and 0.1% Nonidet P-40, followed by SDS-PAGE analysis of the proteins. For enzyme activity assays, the beads were washed three times with lysis buffer.

Chromatin Immunoprecipitation Assay—HeLa cells were transfected with 5 μg of UAS-TK-Luc (25), and 15 μg of the GAL4-VP16-JMJD2A (aa 661–1064) or the parent expression-only GAL4-VP16 control, using the calcium-phosphate method. After 36 h, histones were cross-linked to DNA by adding formaldehyde directly to culture medium to a final concentration of 1%, and incubated for 10 min at 37 °C with mild shaking. Cells were harvested and suspended in lysis buffer (1% SDS, 10 mM EDTA, 50 mM Tris-HCl, pH 8.1) with protease inhibitors. After sonication and dilution of lysates, half of the lysate amount was saved for a no-antibody control, whereas the remaining was incubated over-

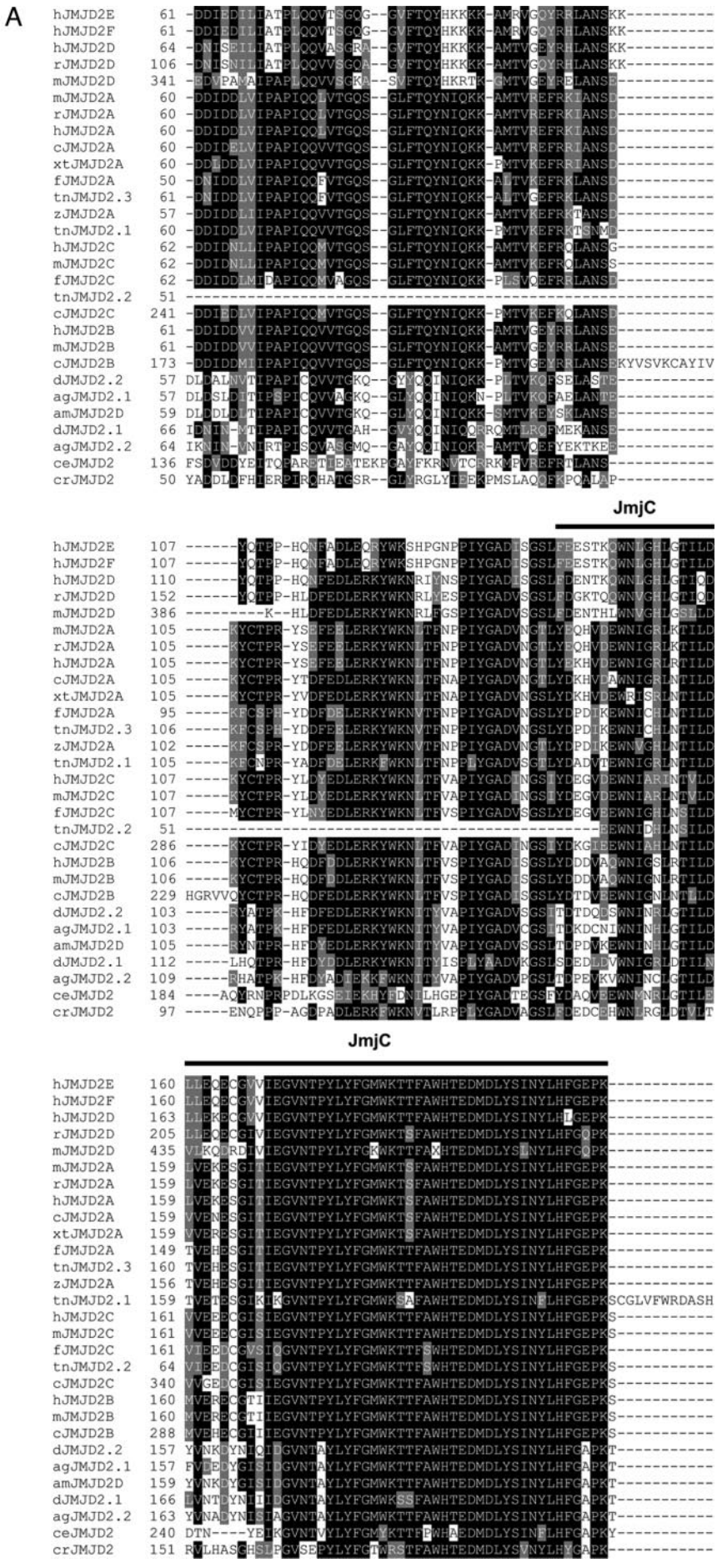

FIG. 1. **Features of the JMJD2 family.** *A*, alignment of JMJD2 protein sequences as identified from public genome data bases (see "Materials and Methods " for accession numbers and supplemental materials for complete alignment). The alignment was carried out using ClustalW, and conserved residues highlighted using Boxshade. Where present, conserved domains are indicated. *B*, neighbor-joining phylogenetic tree of JMJD2 homologs. MEGA3 was used to do bootstrap analysis, protein distance calculation, and tree construction. Bootstrap percentages are presented at each fork. *C*, generalized cartoon showing the conserved domains and elements of JMJD2A. The amino acid locations for each domain as determined using SMART (smart.embl.de) are as follows: JmjN (aa 13–55), JmjC (aa 142–308), PHD 1 (aa 709–767), PHD 2 (aa 829–885), TUDOR 1 (aa 897–954), and TUDOR 2 (aa 955–1011). An alignment of human JMJD2 family members against the region of homology to RBBP2 (aa 185–300) is shown below. *D*, zinc binding activity of JMJD2A. Recombinant proteins were analyzed by SDS-PAGE, transferred to nitrocellulose, incubated with $^{65}ZnCl_2$, washed, and followed by autoradiography (*panel B*). An Amido Black staining of the same gel (*panel A*) is also presented to show the filter-bound proteins from each lane. *Lane 1*, molecular weight markers (note that bovine serum albumin is marked by ^{65}Zn); *lane 2*, GST; *lane 3*, GST-JMJD2A-(661–1064); *Lane 4*, GST-JMJD2A-(710–884).

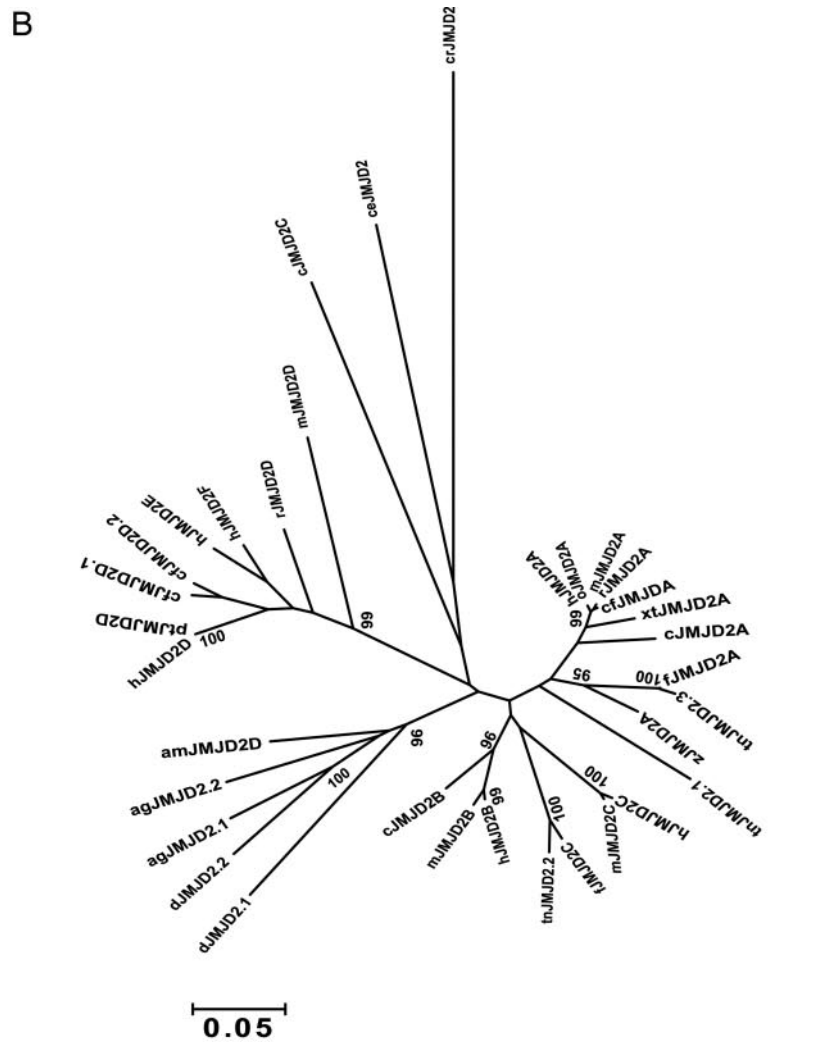

FIG. 1—*continued*

night at 4 °C with an anti-acetyl-histone H3 antibody (Upstate Biotechnology number 06-599). Immunoprecipitated complexes were collected using salmon sperm DNA/protein-agarose. Precipitants were washed, and the immune complex was eluted by adding 250 μl of elution buffer (1% SDS, 0.1 M $NaHCO_3$). Subsequently, 20 μl of 5 M NaCl was added to reverse the formaldehyde cross-linking at 65 °C for 4 h. Following incubation with proteinase K, 0.5 M EDTA, and 1 M Tris-HCl, DNA was recovered by phenol/chloroform and ethanol precipitated. Pellets were suspended in water and subjected to PCR amplification using the TK promoter-specific primers. An input control of 1/100th of the input was removed for use as a positive "input" control, 5′-AGCGTCTTGTCATTGGCGAATTCG-3′, and 5′-TCCTCTAGAGGATAGAATGGCG-3′. The resulting 232-bp product was analyzed by agarose gel electrophoresis.

HDAC Activity Assay—THP-1 cells were grown and collected at a density of 5×10^6. Cells were spun down, washed twice with phosphate-buffered saline, and lysed in 100 μl of lysis buffer (50 nM Tris base, pH 8.0, 150 nM NaCl, 2 mM EDTA, 1% Nonidet P-40, 0.5% Triton X-100) for 30 min at 4 °C with rotation. Lysates were centrifuged at 14,000 × *g* for 30 s at room temperature to pellet insolubles. The supernatant protein aliquots were pre-washed first with 40 μl of protein A-agarose beads rotating at 4 °C for 30 min. After spinning we collected the supernatant and added the antibodies, 2 tubes for each immunoprecipitation. Five μg each of rabbit mock α-FLAG, α-HDAC3, and α-JMJD2A antibodies was added to each aliquot and incubated rotating at 4 °C overnight. We then added 60 μl of agarose beads to each tube and rotated the tubes at 4 °C for 4 h. Beads were spun down at 2000 × *g* for 30 s, and washed 3 times with 500 μl of lysis buffer. We then proceeded to measure the HDAC activity of each immunoprecipitate following the two-step method of the CycLex quantitative test kit (MBL, Watertown, MA). Each immunoprecipitation included controls with and without 5 μM trichostatin A (TSA). Ten μl of each immunoprecipitate was incubated with 5–15 μl of assay buffer (20 nM Tris-HCl, pH 8.0, 125 mM NaCl, 1% glycerol) and 25 μl of 2× fluoro-substrate peptide (40 μM) for 20 min. We then added 50 μl of HDAC stop solution (1 milli-absorbance unit/ml of lysyl endopeptidase and 2 μM trichostatin A) to each well, and incubated the wells for 20 min at room temperature. Finally, the fluorescence intensity was measured using a Wallac 1420 work station with excitation at 380 nm and emission at 480 nm.

Propidium Iodide Fluorescence-activated Cell Sorter Cell Cycle Analysis—Propidium iodide-fluorescence-activated cell sorter cell cycle analysis was done as previously described (23).

RESULTS

Isolation of JMJD2A and Identification of Its Homologs—During the screening of a human fetal liver cDNA library for cloning genes related to the transcription factor Sp1 superfamily, we isolated a 3169-nucleotide positive clone, designated λHFLSP5, which contained two open reading frames fused in-frame and separated by stop codons. The 3′ open reading frame corresponded to amino acids 324–480 of the Sp1 superfamily member, transforming growth factor-β-inducible protein TIEG (26), whereas the 5′ open reading frame coded for a novel protein. Whereas the functional characterization of this protein was in progress, the randomly cloned cDNA KIAA0677 was published (27), encoding a hypothetical 1064-residue protein of unknown function. This was subsequently described as the first member of the JMJD2 family by Katoh (15). Sequence similarity searches showed that the 5′ open reading frame of clone λHFLSP5 corresponded to amino acids 661–1064 of the KIAA0677-encoded protein, with only one amino acid difference existing between the two proteins (λHFLSP5 codes for threonine at position 859, whereas KIAA0677 codes for serine). Data base searches for other proteins with homology to KIAA0677 identified two other homologs that have subsequently been called JMJD2B and JMJD2C. JMJD2C has also been named GASC-1, and is amplified in squamous cell carcinoma (28), indicating that this family of proteins may play critical roles in carcinogenesis. LocusLink analysis indicated that the three cDNAs have been mapped to the following locations, JMJD2A to 1p34.1, JMJD2B to 19p13.3, and JMJD2C to 9p24-p23. Examination of the completed genomes of mouse and fugu identified homologs in each genome. Katoh (15) identified three additional JMJD2 open reading frames on chromosome 11q21, and data base searching has identified several homologs of the JMJD2 family in various organisms. A partial alignment of all identified proteins is shown in Fig. 1*A*, and a full alignment is provided as supplementary information. The presence of these homologs within the human, mouse, and fugu genomes indicates a strong evolutionary selection for this gene, and that these genes were shared by a common ancestor prior to the divergence of teleosts and mammals 450 million years ago. A phylogenetic analysis of the JMJD2 family is also shown graphically in Fig. 1*B*.

Several of these identified homologs contain divergent features (*e.g.* mJMJD2D has a >250-aa extension at the 5′-end of its protein, whereas tnJMJD2.1 has a 95-aa insertion, and chicken JMJD2B has a 52-aa insert within the protein plus a 230-aa 3′ extension that is not observed in any other of the JMJD2 family members). In addition, many of the distant homologs are truncated (*e.g.* amJMJD2D is 328 aa compared with hJMJD2D, which is 523 aa). It must be noted that some of the proteins used in this analysis, including cJMJD2B, are predicted proteins from genome assemblies, and may contain errors.

One feature that emerges from this analysis is that the most significantly conserved region is the N-terminal. Indeed JMJDs D–F appear to be truncated forms of the JMJD2 family, and this also appears to be so for many of the lower animal sequences.

Using CDART, analysis of KIAA0677, KIAA0780, and KIAA0876 revealed the presence of several structural elements. Two LAP/PHD zinc fingers, one JmjN, one JmjC (containing an internal retinoblastoma-binding protein 2 (RBBP2)-like sequence), and two Tudor domains are shown diagrammatically in Fig. 1*C*. An alignment of the human JMJD2 family members plus hRBBP2 is also shown. The LAP/PHD-1 domain contains a typical PHD consensus sequence Cys_4-His-Cys_3, whereas the LAP/PHD-2 domain has a conserved, yet atypical PHD motif Cys_5-His-Cys_2-His. The JMJD2A region 767–868 immediately following the LAP/PHD-1 finger has also been referred to as the PER domain because it is conserved in peregrin (also known as BR140) (Fig. 1*C*) and other eukaryotic proteins (29). The entire JMJD2A cysteine-rich region encompassing the LAP/PHD fingers (residues 710–884) shares significant sequence similarity with corresponding domains of human proteins AF10 and AF17, which are involved in leukemia-associated translocations (30, 31), as well as proteins from other organisms, including *M. musculus*, *D. melanogaster*, *A. gambiae*, *Arabidopsis thaliana*, *C. elegans*, *S. pombe*, and *S. cerevisiae* (data not shown). The evolutionary conservation of this region in several diverse proteins from yeast to human suggests that this protein domain performs a critical function. To determine whether the JMJD2A LAP/PHD zinc fingers are functional, we assessed whether they had the ability to bind zinc ions, by using an *in vitro* ^{65}Zn binding assay. This analysis showed that bacterially produced fusion proteins GST-JMJD2A-(661–1064) and GST-JMJD2A-(710–884) bound ^{65}Zn (Fig. 1*D*, *panel B*, *lanes 3* and 4), whereas GST alone did not (Fig. 1*D*, *panel B*, *lane 2*), demonstrating that JMJD2A comprises a functional zinc-coordinating module(s). It must be noted that Clissold and Ponting (32) have also indicated that the JMJC domain may also be capable of binding zinc. We did not test this possibility.

Expression and Distribution of JMJD2A in Human Tissues and Cell Lines—To examine the expression of JMJD2A we probed a panel of human tissues and cell lines by Northern blot analysis (Fig. 2*A*). In the human tissues examined, *JMJD2A* mRNA was observed in all tissues with the lowest expression in skeletal muscle and highest in lung. To assess the expression of *JMJD2A* in more detail, we designed, and ran, RT-PCR in a

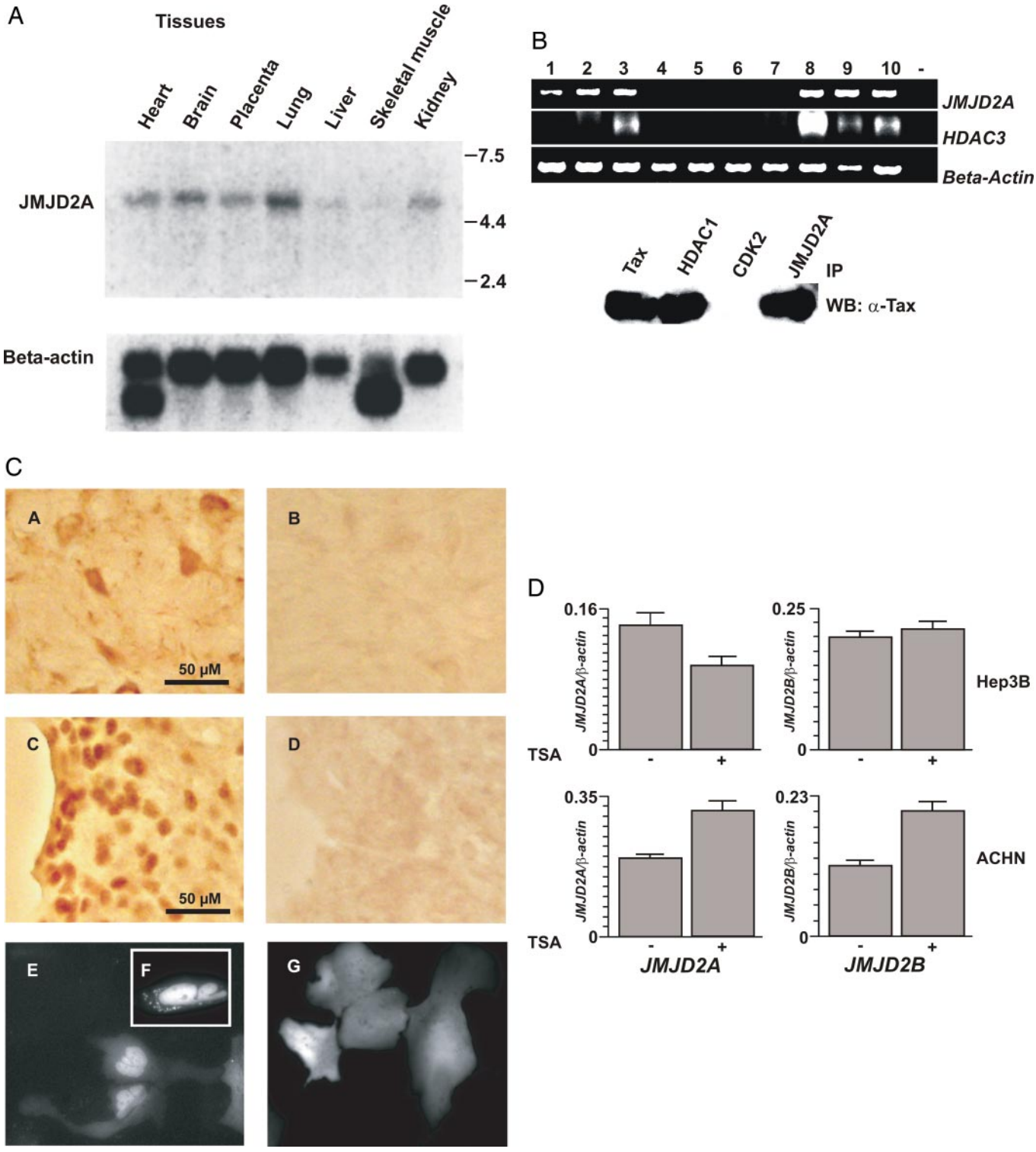

FIG. 2. **Expression and distribution of JMJD2A.** *A*, multiple tissue Northern blot analysis shows that *JMJD2A* is widely expressed in human tissues. The blot was hybridized with a *JMJD2A*-specific radiolabeled probe and subsequently with a β-actin probe. *B*, RT-PCR analysis of *JMJD2A and HDAC3* and immunoprecipitation of Tax. RT-PCR analysis was carried out on the following cell lines: *lane 1*, HTLV-1-infected HUT102; *lane 2*, HTLV-1-infected C81; *lane 3*, HTLV-1-infected T-cell clone 1; *lane 4*, HTLV-1-infected T-cell clone 2; *lane 5*, T-cell clone 1; *lane 6*, T-cell clone 2; *lane 7*, Epstein-Barr virus B cell; *lane 8*, HT1376; *lane 9*, THP1; *lane 10*, U2OS. *Lower panel*, cellular protein extracts were immunoprecipitated with the indicated antibodies (Tax, HDAC1, CDK2 and JMJD2A), and a protein gel was run, followed by Western blots with an anti-Tax antibody. *C*, immunocytochemistry (*ICC*) showing JMJD2A and JMJD2B immunoreactivity in rat brain. ICC for JMJD2A and JMJD2B in the medulla was performed using adjacent sections. JMJD2A (*panel A*) immunoreactivity is located in both the nucleus and cytoplasm, whereas that of JMJD2B (*panel C*) is primarily located in the nucleus. The results of preimmune serum are shown alongside (*panels B* and *D*). Nuclear localization of JMJD2A fused to EYFP in HEK-293T cells is shown (*panels E-G*). *Panel E* shows the predominantly nuclear distribution of the EYFP-N1 JMJD2A fusion. In the *inset* (*panel F*), some intracellular distribution is observed. The EYFP-N1 control is distributed homogeneously and nonspecifically throughout the cell (*panel G*). *D*, RPA analysis of *JMJD2A* and *JMJD2B* expression in Hep3B and ACHN cells cultured in the presence or absence of TSA. The *y* axis values represent arbitrary numbers for each gene normalized to *β-actin*, expressed as the ratio between *gene/β-actin*. The values shown are the mean ± S.E. for three separate experiments.

series of cell lines. Several cell lines showed little or no expression of *JMJD2A*. However, good expression levels of JMJD2A mRNA were observed in 3 of 4 human T-cell lymphotropic virus (HTLV-1)-infected cell lines. High expression was also found in other non-infected cell lines, including the HT1376 bladder carcinoma cell line and the U2OS osteosarcoma cell line (Fig. 2*B*). Interestingly, HDAC3 mRNA was only detected in cell lines that had detectable JMJD2A mRNA expression. A protein critical for the regulation of HTLV-1 is the transcriptional oncoprotein Tax. This protein has been shown to functionally associate with HDAC1 (33, 34), and we have shown that it also binds HDAC3.[2] Using an immunoprecipitation approach in the HTLV-1-infected cell line C81, we were able to demonstrate that Tax also associates with JMJD2A (Fig. 2*B*). When JMJD2A was overexpressed in these cells, the expression of Tax mRNA was down-regulated 24 h post-transfection, indicating that JMJD2A may function to regulate the expression of Tax (data not shown).

JMJD2A has a potential bipartite nuclear localization signal spanning residues 999–1015 and overlapping with the Tudor-2 domain. To verify intracellular localization of JMJD2s, we raised antibodies to JMJD2A and JMJD2B and first performed immunohistochemistry analysis in rat brain tissue (medulla and pons). Nuclear staining was observed for JMJD2A and JMJD2B, indicating that they may play important regulatory roles within the nucleus (Fig. 2*C*, *panels A–D*). The fusion of JMJD2A to EYFP also demonstrated predominantly nuclear expression in HEK-293T cells, although diffuse intracellular localization was observed in some cells, whereas the original EYFP has a universal distribution within the cell (Fig. 2*C*, *panels E–G*).

The expression of many genes has been shown to be regulated at the chromatin level (1). We therefore examined whether the expression of *JMJD2A* and *JMJD2B* was altered following treatments of various cell lines with the HDAC inhibitor trichostatin A. Cell type-dependent differential responses to TSA were observed, whereby expression of *JMJD2A* was down-regulated, whereas that of *JMJD2B* was unaffected in the liver-specific cell line Hep3B. In contrast, both genes were up-regulated in the renal cell carcinoma cell line ACHN (Fig. 2*D*). This is not an unexpected result as we have previously observed tissue-specific responses to HDAC inhibitors (22, 35–37). The results support the concept of a wide variability in JMJD2 family function that is cell type-specific.

JMJD2A Associates with Class I HDACs and Directs HDAC-mediated Repression both in Vitro and in Vivo—JMJD2A contains two domains with the potential to interact with HDACs, the LAP/PHD fingers (38), and the Tudor domains (39). Therefore we sought to address the question whether JMJD2A also interacts with HDACs and participates in chromatin-mediated gene regulation.

Using *in vitro*-translated [^{35}S]methionine-labeled JMJD2A we observed that it was able to bind to immobilized recombinant GST-HDAC1, GST-HDAC2, and GST-HDAC3 fusion proteins (data not shown). Immunoprecipitation experiments also showed that native JMJD2A was not a member of the classical mSin3-HDAC complex in THP-1 cells as it could be precipitated along with HDAC1 and HDAC3, but not with mSin3 (Fig. 3*A*).

Because the 661–1064 half of JMJD2A contains the LAP/PHD and Tudor domains that constitute potential HDAC-binding sites, we tested its ability to inhibit activated transcription, using a vector expressing the fusion protein GAL4-VP16-JMJD2A-(661–1064), as described previously for other repressors (40). Importantly, JMJD2A-(661–1064) strongly inhibited the VP16-activated transcription in 293 cells (Fig. 3*B*), and this effect was partially abolished upon HDAC inhibition with TSA, indicating that the observed effect is HDAC-dependent.

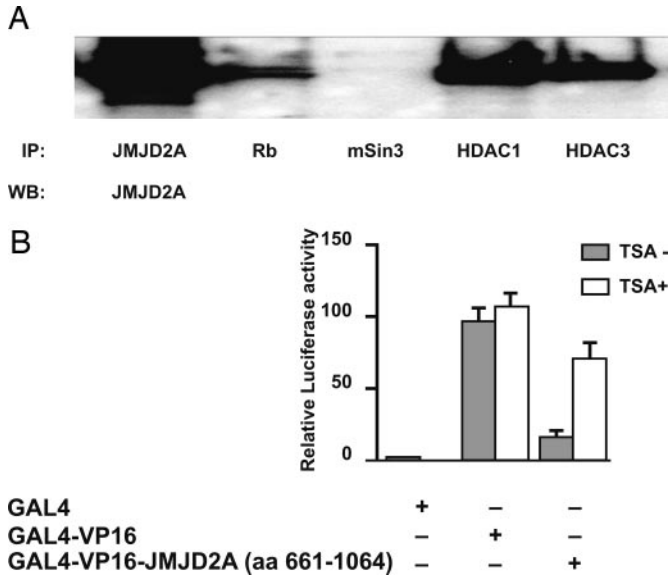

FIG. 3. **JMJD2A associates with class I HDACs and directs HDAC-mediated repression.** *A*, immunoprecipitation of native JMJD2A by various antibodies to classical HDAC containing complexes. Proteins were immunoprecipitated (*IP*) with various specific antibodies, run on Western blots (*WB*), and probed with antibodies to the native JMJD2A protein. *B*, TSA-sensitive repression of activated transcription by JMJD2A. UAS-TK-Luc was transiently cotransfected into 293 cells with GAL4, GAL4-VP16, or GAL4-VP16-JMJD2A (aa 661–1064). Following recovery, transfected cells were cultured in the absence (*white bars*) or presence (*shaded bars*) of 100 nM TSA for 24 h. Relative luciferase activity was subsequently measured. The experiment was performed in triplicate and is presented as the mean ± S.E.

To demonstrate that JMJD2A recruits HDACs *in vivo*, we used a chromatin immunoprecipitation assay to determine the level of histone acetylation at a promoter repressed by JMJD2A (aa 661–1064) (Fig. 4*A*). This analysis showed that GAL4-JMJD2A (aa 661–1064) expression resulted in a dramatic decrease of histone H3 acetylation at the TK promoter, and this effect was partially reversed upon treatment with TSA. The correlation between the JMJD2A-mediated repression (Fig. 3*B*) and decreased histone acetylation at the target promoter (Fig. 4*A*) provides strong evidence that the JMJD2A-directed repression is HDAC-mediated. Next, we investigated whether JMJD2A exists in a protein complex that retains functional HDAC enzymatic activity, by a combined immunoprecipitation/HDAC activity assay (Fig. 4*B*). Our results indicate that JMJD2A antibodies immunoprecipitate significant HDAC activity.

JMJD2A Association with pRb Mediates Repression of E2F-responsive Promoters—Based on the fact that RBBP1 contains one Tudor domain, RBBP2 contains three LAP/PHD domains, and RBBP2 shares sequence similarity with JMJD2A over their JmjN and JmjC domains (Fig. 1*C*), we reasoned that JMJD2A might also interact with pRb. Immunoprecipitation with antibodies to pRb and subsequent Western blotting with JMJD2A antibody revealed a potential association (Fig. 3*A*). Using a mammalian two-hybrid system we sought to investigate which regions of JMJD2A interact with pRb *in vivo* (Fig. 5*A*). Cotransfection of constructs expressing AD-fused JMJD2A cDNA fragments and GAL4-pRb-BD into 293 cells activated the reporter to a level comparable with that of SV40-AD (Fig. 5*A*), and was especially prominent for the Tudor domain interaction, indicating an association between pRb and various do-

[2] R. Villanueva, A. H. Iglesias, S. Camelo, S. G. Gray, L. C. Sanin, and F. Dangond, unpublished data.

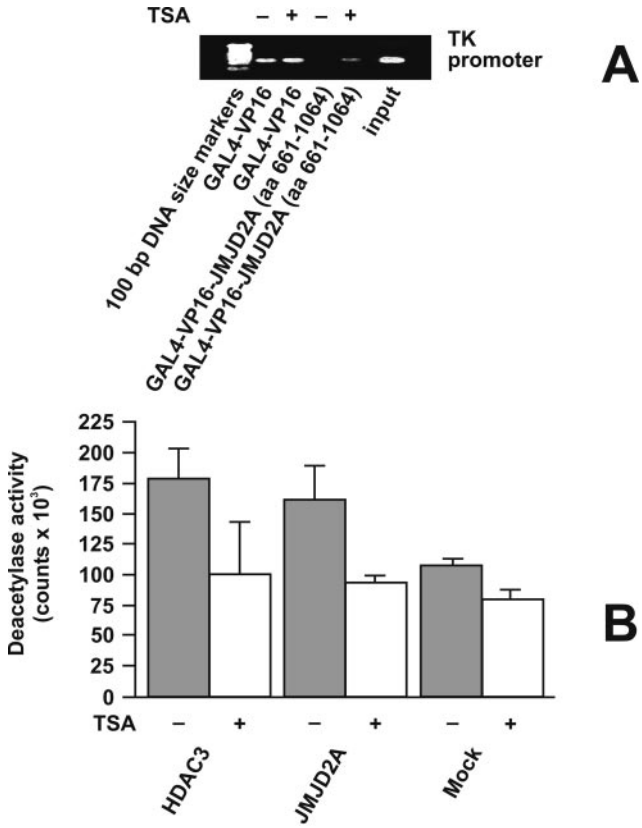

FIG. 4. **JMJD2A associates with HDAC activity *in vivo*.** *A*, chromatin immunoprecipitation assay demonstrating decreased histone acetylation locally at a target promoter as a consequence of JMJD2A expression, which is sensitive to TSA derepression. Vectors expressing GAL4-VP16 and GAL4-VP16-JMJD2A (aa 661–1064) were cotransfected along with the reporter plasmid UAS-TK-Luc into 293 cells. Transfected cells were subsequently cultured in the presence or absence of 100 nM TSA for 24 h. Subsequently, chromatin immunoprecipitation with antibodies to acetylated histone H3 was performed and the acetylation status of chromatin assembled on the TK promoter was assayed by PCR as described under "Materials and Methods." The *first lane* is a standard molecular weight marker, whereas *input* represents a positive control consisting of $1/100^{th}$ of the original fixed chromatin prior to immunoprecipitation. *B*, JMJD2A immunoprecipitates HDAC activity, indicating that it exists in a complex with HDACs that retain enzymatic function. Note the positive control activity immunoprecipitated by antibodies to HDAC3.

mains of JMJD2A *in vivo*. However, each region was found to associate to some degree, indicating that perhaps a complex involving pRb, JMJD2A, and various other bridging proteins may be assembled at the promoter. Additional evidence supporting the notion of a pRb-JMJD2A complex came from immunoprecipitation-Western blot experiments with FLAG-tagged constructs. These experiments showed that JMJD2A also bound pRb, and that the A/B pocket was required for binding, but was not essential, because the pRbΔ22 mutant cotransfected with JMJD2A retained some binding (Fig. 5*B*). Along with our findings that *in vitro* translated [^{35}S]methionine-labeled JMJD2A bound to immobilized recombinant GST-pRb (data not shown), and that native JMJD2A could be immunoprecipitated with antibodies to pRb (Fig. 3*A*), this data demonstrates that JMJD2A interacts with pRb both *in vitro* and *in vivo*. Finally, because pRb can assemble transcription repression complexes at E2F-regulated promoters (9–12), we used an E2F promoter luciferase fusion construct to examine whether JMJD2A can direct repression from E2F promoters. JMJD2A was found to repress activity of a dihydrofolate reductase-luciferase E2F-target promoter to levels that were comparable with those of pRb alone (Fig. 6), and synergistically enhances repression when combined with pRb ($p < 0.05$), indicating that JMJD2A directs repression of E2F responsive promoters.

DISCUSSION

In this paper we utilized traditional screening approaches coupled with bioinformatic analysis to identify an evolutionarily conserved gene family, now referred to as JMJD2. These proteins contain two Jmj domains, two LAP/PHD zinc fingers, and two Tudor domains. JmjC motifs have been described recently in eukaryotic proteins involved in chromatin-mediated transcriptional regulation of gene expression (32). In addition, both LAP/PHD and Tudor domains have also been implicated in protein-protein interactions involving chromatin remodeling complexes, in particular HDAC-containing complexes (38, 39). Tudor domains are modules of unknown structure and function that have been described in a small number of proteins that participate in RNA-binding and gene regulation (41). In *Drosophila*, the *tudor* protein contains multiple copies of the Tudor motifs and is required during oogenesis for the formation of primordial germ cells and for normal abdominal segmentation (42). Remarkably, only 9 genes encoding Tudor domain-containing proteins have been identified in the entire human genome (43). LAP/PHD fingers are found in diverse proteins from yeast to human, suggesting conservation of an important function. Notably, the pRb-binding protein RBBP2 has JmjN, JmjC, and LAP/PHD motifs but lacks Tudor domains, whereas RBBP1, which is involved in pRb-mediated repression through HDAC-dependent and -independent mechanisms (14), has one Tudor domain but no LAP/PHD zinc fingers or Jmj domains. Interestingly, JMJD2A contains all three classes of these structural motifs. The presence of LAP/PHD, JmjN, JmjC, and Tudor domains in three proteins that interact with pRb is intriguing, and suggests that these protein modules may all play important roles in the mechanisms of pRb function.

We have shown that JMJD2A associates with members of the class I HDACs. Functional studies demonstrated that the region encompassing amino acids 661–1064 of JMJD2A, which contained both the LAP/PHD and Tudor domains, was the minimum region necessary to associate direct repression possibly because of its ability to recruit both pRb and HDACs.

Treatments with the HDAC inhibitor TSA alleviated JMJD2A-mediated repression, further indicating that this protein functions by targeting HDACs to its target genes. To confirm this we utilized a chromatin immunoprecipitation strategy to show that at a promoter construct targeted by JMJD2A, levels of acetylated histone H3 were dramatically decreased. Taken together, the data presented demonstrate that the JMJD2 proteins are another family of proteins that utilize HDACs at their target promoters.

In addition to associating with HDACs, the domain structure of these proteins indicated that JMJD2s may also associate with pRb, a critical regulator of the cell cycle (6, 44). We demonstrated that this is in fact the case. Immunoprecipitation with antibodies to pRb pulled down native JMJD2A, and mammalian two-hybrid assays demonstrated that this interaction could occur *in vivo*.

The binding of JMJD2A to pRb raised the question whether this interaction is mediated through the L*X*C*X*E-binding site in the pRb A/B pocket. Sequence analysis revealed that JMJD2A lacks an L*X*C*X*E or I*X*C*X*E element but it contains regions resembling this motif, including the sequences FNCAE (residues 283–287) in the JmjC domain, and EECPE (residues 367–371), RVCLE (residues 400–404), and LKCIF (residues 828–832), the latter at the beginning of the LAP/PHD-2 domain. Using the mammalian two-hybrid system we tested various fragments of JMJD2A for their ability to associate with

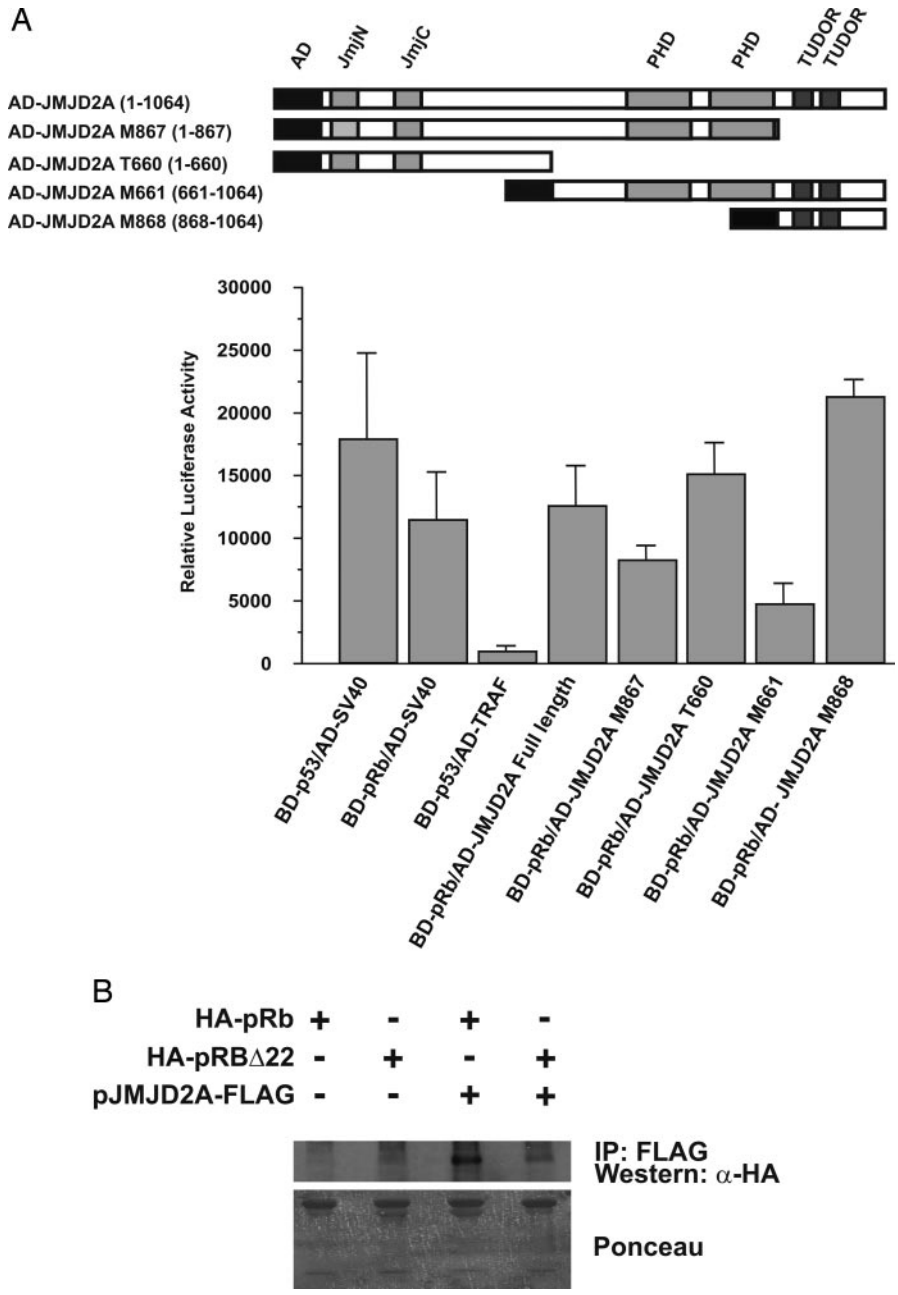

FIG. 5. ***In vivo*** **association of JMJD2A with pRb.** *A*, a mammalian two-hybrid system was used to identify the regions of JMJD2A that associate with pRb. Constructs expressing the NF-κB AD fused to the indicated protein fragments and plasmids expressing the GAL4 DNA-binding domain (*BD*) fused with pRb were cotransfected into 293 cells along with the GAL4-binding site encoding pFR-Luc reporter plasmid. Positive (BD-p53/AD-SV40 and BD-pRb/AD-SV40) and negative (BD-p53/AD-TRAF) interaction controls were included. The experiment was performed in triplicate and relative luciferase activity is presented as the mean ± S.E. *B*, HA-tagged pRb A/B pocket mutant also retains some ability to bind JMJD2A in immunoprecipitation (*IP*) experiments with FLAG-tagged JMJD2A.

pRb. The constructs included fragments containing solely the Jumonji domains (fragment Thr-660 corresponding to residues 1–660 of the full-length JMJD2A), a fragment containing the Jmj and PHD domains (fragment Met-867, corresponding to residues 1–867), a fragment containing the PHD and Tudor domains (Met-661, corresponding to residues 661–1064), and a fragment containing only the Tudor domains (Met-868, corresponding to residues 868–1064). These results showed that all fragments had the ability to associate with pRb and transactivate expression of luciferase to some degree. It is therefore possible that JMJD2A participates in the pRb-mediated regulation of E2F-dependent promoters preceding or following the S phase. We were also able to confirm that JMJD2A was able to directly regulate the expression of an E2F responsive promoter.

These results overall indicate that the association of E2F, pRb, JMJD2A, and HDACs 1–3 may be more complex than through direct interactions, and may involve bridging proteins. This is not an unusual situation for chromatin modifying complexes involving pRb, E2F, and HDACs.

Recently, the HP1 protein containing a "Chromo" domain (a domain that shares strong similarities to Tudor domains), has been shown to associate with pRb and E2F to direct repression (45, 46). More recently 53BP1, a protein containing tandem Tudor domains similar to JMJD2A has been shown to bind directly to methylated lysine 79 on histone H3 at double-stranded DNA breaks (47). This would indicate that perhaps JMJD2A may also bind methylated histones, or acts as a bridge for proteins that recruit histone methyltransferases, pRB and E2F. Indeed the region of the ERG (*ets*-related gene) histone methyltransferase that has been shown to form a complex with mSin3A/mSin3B and HDAC1/2 contains a Tudor domain. Leaving aside the Tudor domains, a recent report has shown that the yeast homolog of RBBP2 binds HDACs through its PHD fingers (48). Another Rb-binding protein, RBBP1, has also been shown to form bridging complexes to recruit HDACs to Rb/E2F complexes (14), but although it contains both a Tudor and a Chromo domain, these domains are not involved with the association to HDACs. Finally, a recent report in plants has

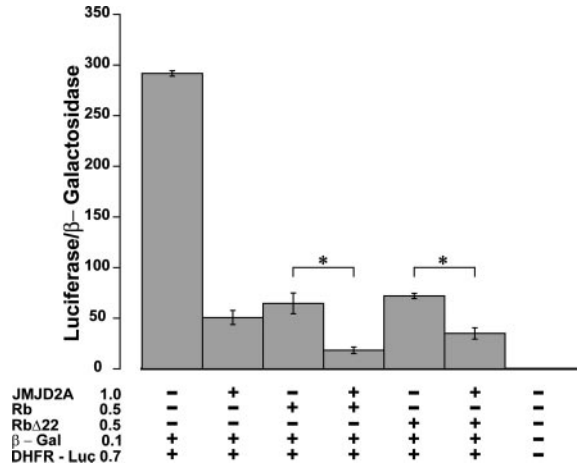

FIG. 6. **JMJD2A represses E2F responsive promoters.** 293 cells were transfected with the plasmids at concentrations shown (μg/ml). Cells were harvested 48 h post-transfection, and luciferase and β-galactosidase expression were measured using the Dual Light® luminescent reporter gene assay system. Values of luciferase were normalized against β-galactosidase. The results are graphed as the mean ± S.E. of three independent experiments. A Student's *t* test was used to test for significance ($p < 0.05$) as indicated by *asterisks*.

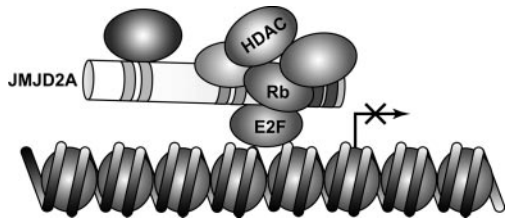

FIG. 7. **Stylized cartoon showing the hypothesized interactions between the various domains of JMJD2A, pRb, E2F, and additional potential members of a JMJD2A histone modifying complex.** Molecules are not depicted at comparative size.

indicated that some plant jumonji transcription factors have associated histone modifying activity (49). Overall this data confirms our observations from the mammalian two-hybrid assays, and indicate that all three types of domains can be associated with proteins that serve to recruit or interact with pRb. A stylized cartoon depicting the potential chromatin bound complex involving JMJD2A, HDACs, pRb, and E2F is shown in Fig. 7.

Several groups have demonstrated the importance of HDACs in pRb-mediated repression (10–12). Although the molecular mechanisms of pRb-mediated transcriptional repression are currently unknown, they are likely to be complex, involving both masking of the E2F transactivation domain and chromatin-mediated repression (5, 7). Because JMJD2A interacts physically with recombinant pRb, HDAC1, HDAC2, and HDAC3, it is conceivable that it may serve as a bridging molecule facilitating the assembly of complexes containing pRb, HDACs, and possibly other corepressors, on E2F-regulated promoters. The presence of protein-protein interaction motifs, such as Tudor domains, in JMJD2A further suggests other associations.

For example, the survival motor neuron 1 (SMN1) gene product has been shown to be involved in the assembly of a large complex (termed the SMN complex) that promotes the formation of spliceosomal U small nuclear ribonucleoproteins. It is the Tudor domain of SMN that interacts with spliceosomal (Sm) proteins (50). As such we feel that JMJD2A family members may participate in other protein interactions and/or protein complexes.

An interesting finding in our study has been the higher expression of JMJD2A in HTLV-1-infected cell lines. The HTLV-1 protein Tax has been shown to mediate cell cycle dysregulation and promote the transcriptional activation of its own mRNA by binding to the histone acetyltransferase CREB-binding protein (CBP)/P300 (2). By overexpressing JMJD2A in a HTLV-1-infected cell line, we were able to down-regulate the expression of Tax.[3] JMJD2A may thus function to recruit HDACs to the HTLV-1 promoter to regulate the expression of Tax.

In conclusion, this work identifies JMJD2A as a novel interaction partner of pRb, class I HDACs, and Tax, and provides insights into pRb repression mechanisms. Although the physiological function of the JMJD2A protein is not currently known, our findings support the notion that JMJD2A plays an important role in cell cycle regulation and the transformation process through its association with pRb/HDACs and the viral transactivator Tax, and its effects on chromatin-mediated gene regulation.

Acknowledgments—We thank William Kaelin, Jr., Takahiro Nagase, Stuart L. Schreiber, and Edward Seto for kindly providing constructs. We thank Dr. John A. A. Ladias for the kind gift of constructs and critical input into this work.

REFERENCES

1. Gray, S. G., and Ekström, T. J. (2001) *Exp. Cell Res.* **262,** 75–83
2. Gray, S. G., and Teh, B. T. (2001) *Curr. Mol. Med.* **1,** 401–429
3. Gao, L., Cueto, M. A., Asselbergs, F., and Atadja, P. (2002) *J. Biol. Chem.* **277,** 25748–25755
4. Liu, H., Dibling, B., Spike, B., Dirlam, A., and Macleod, K. (2004) *Curr. Opin. Genet. Dev.* **14,** 55–64
5. Stevaux, O., and Dyson, N. J. (2002) *Curr. Opin. Cell Biol.* **14,** 684–691
6. Harbour, J. W., and Dean, D. C. (2000) *Nat. Cell Biol.* **2,** E65-E67
7. Harbour, J. W., and Dean, D. C. (2000) *Genes Dev.* **14,** 2393–2409
8. Ross, J. F., Liu, X., and Dynlacht, B. D. (1999) *Mol. Cell* **3,** 195–205
9. Meloni, A. R., Smith, E. J., and Nevins, J. R. (1999) *Proc. Natl. Acad. Sci. U. S. A.* **96,** 9574–9579
10. Magnaghi-Jaulin, L., Groisman, R., Naguibneva, I., Robin, P., Lorain, S., Le Villain, J. P., Troalen, F., Trouche, D., and Harel-Bellan, A. (1998) *Nature* **391,** 601–605
11. Luo, R. X., Postigo, A. A., and Dean, D. C. (1998) *Cell* **92,** 463–473
12. Brehm, A., Miska, E. A., McCance, D. J., Reid, J. L., Bannister, A. J., and Kouzarides, T. (1998) *Nature* **391,** 597–601
13. Lai, A., Lee, J. M., Yang, W. M., DeCaprio, J. A., Kaelin, W. G., Jr., Seto, E., and Branton, P. E. (1999) *Mol. Cell. Biol.* **19,** 6632–6641
14. Lai, A., Kennedy, B. K., Barbie, D. A., Bertos, N. R., Yang, X. J., Theberge, M. C., Tsai, S. C., Seto, E., Zhang, Y., Kuzmichev, A., Lane, W. S., Reinberg, D., Harlow, E., and Branton, P. E. (2001) *Mol. Cell. Biol.* **21,** 2918–2932
15. Katoh, M. (2004) *Int. J. Oncol.* **24,** 1623–1628
16. Ladias, J. A. A. (1994) *J. Biol. Chem.* **269,** 5944–5951
17. Green, V. J., Kokkotou, E., and Ladias, J. A. A. (1998) *J. Biol. Chem.* **273,** 29950–29957
18. Sellers, W. R., Novitch, B. G., Miyake, S., Heith, A., Otterson, G. A., Kaye, F. J., Lassar, A. B., and Kaelin, W. G., Jr. (1998) *Genes Dev.* **12,** 95–106
19. Yang, W. M., Yao, Y. L., Sun, J. M., Davie, J. R., and Seto, E. (1997) *J. Biol. Chem.* **272,** 28001–28007
20. Kumar, S., Tamura, K., and Nei, M. (2004) *Brief Bioinform.* **5,** 150–163
21. Letunic, I., Copley, R. R., Schmidt, S., Ciccarelli, F. D., Doerks, T., Schultz, J., Ponting, C. P., and Bork, P. (2004) *Nucleic Acids Res.* **32,** D142–144
22. Gray, S. G., and Ekström, T. J. (1998) *Biochem. Biophys. Res. Commun.* **245,** 423–427
23. Dangond, F., Hafler, D. A., Tong, J. K., Randall, J., Kojima, R., Utku, N., and Gullans, S. R. (1998) *Biochem. Biophys. Res. Commun.* **242,** 648–652
24. Koibuchi, N., Gibbs, R. B., Suzuki, M., and Pfaff, D. W. (1991) *Endocrinology* **129,** 3208–3216
25. Heinzel, T., Lavinsky, R. M., Mullen, T. M., Soderstrom, M., Laherty, C. D., Torchia, J., Yang, W. M., Brard, G., Ngo, S. D., Davie, J. R., Seto, E., Eisenman, R. N., Rose, D. W., Glass, C. K., and Rosenfeld, M. G. (1997) *Nature* **387,** 43–48
26. Subramaniam, M., Harris, S. A., Oursler, M. J., Rasmussen, K., Riggs, B. L., and Spelsberg, T. C. (1995) *Nucleic Acids Res.* **23,** 4907–4912
27. Ishikawa, K., Nagase, T., Suyama, M., Miyajima, N., Tanaka, A., Kotani, H., Nomura, N., and Ohara, O. (1998) *DNA Res.* **5,** 169–176
28. Yang, Z.-Q., Imoto, I., Fukuda, Y., Pimjhaokham, A., Shimada, Y., Imamura, M., Sugano, S., Nakamura, Y., and Inazawa, J. (2000) *Cancer Res.* **60,** 4735–4739
29. Balciunas, D., and Ronne, H. (2000) *Trends Biochem. Sci* **25,** 274–276
30. Chaplin, T., Ayton, P., Bernard, O. A., Saha, V., Della Valle, V., Hillion, J., Gregorini, A., Lillington, D., Berger, R., and Young, B. D. (1995) *Blood* **85,** 1435–1441

[3] S. G. Gray, A. H. Iglesias, F. Lizcano, R. Villanueva, S. Camelo, H. Jingu, B. T. Teh, N. Koibuchi, W. W. Chin, E. Kokkotou, and F. Dangond, unpublished observations.

31. Prasad, R., Leshkowitz, D., Gu, Y., Alder, H., Nakamura, T., Saito, H., Hebner, K., Berger, R., Croce, C. M., and Canaani, E. (1994) *Proc. Natl. Acad. Sci. U. S. A.* **91,** 8107–8111
32. Clissold, P. M., and Ponting, C. P. (2001) *Trends Biochem. Sci.* **26,** 7–9
33. Ego, T., Ariumi, Y., and Shimotohno, K. (2002) *Oncogene* **21,** 7241–7246
34. Lu, H., Pise-Masison, C. A., Linton, R., Park, H. U., Schiltz, R. L., Sartorelli, V., and Brady, J. N. (2004) *J. Virol.* **78,** 6735–6743
35. Gray, S. G., Qian, C. N., Furge, K., Guo, X., and Teh, B. T. (2004) *Int. J. Oncol.* **24,** 773–795
36. Gray, S. G., Iglesias, A. H., Teh, B. T., and Dangond, F. (2003) *Gene Expr.* **11,** 13–21
37. Gray, S. G., Yakovleva, T., Hartmann, W., Tally, M., Bakalkin, G., and Ekström, T. J. (1999) *Exp. Cell Res.* **253,** 618–628
38. Zhang, Y., LeRoy, G., Seelig, H.-P., Lane, W. S., and Reinberg, D. (1998) *Cell* **95,** 279–289
39. Yang, L., Mei, Q., Zielinska-Kwiatkowska, A., Matsui, Y., Blackburn, M. L., Benedetti, D., Krumm, A. A., Taborsky, G. J., Jr., and Chansky, H. A. (2002) *Biochem. J.* **369,** 651–657
40. Hassig, C. A., Tong, J. K., Fleischer, T. C., Owa, T., Grable, P. G., Ayer, D. E., and Schreiber, S. L. (1998) *Proc. Natl. Acad. Sci. U. S. A.* **95,** 3519–3524
41. Ponting, C. P. (1997) *Trends Biochem. Sci.* **22,** 51–52
42. Golumbeski, G. S., Bardsley, A., Tax, F., and Boswell, R. E. (1991) *Genes Dev.* **5,** 2060–2070
43. Venter, J. C., Adams, M. D., Myers, E. W., Li, P. W., Mural, R. J., Sutton, G. G., Smith, H. O., Yandell, M., Evans, C. A., Holt, R. A., Gocayne, J. D., Amanatides, P., Ballew, R. M. *et al.* (2001) *Science* **291,** 1304–1351
44. Kaelin, W. G., Jr. (1999) *Bioessays* **21,** 950–958
45. Nielsen, S. J., Schneider, R., Bauer, U. M., Bannister, A. J., Morrison, A., O'Carroll, D., Firestein, R., Cleary, M., Jenuwein, T., Herrera, R. E., and Kouzarides, T. (2001) *Nature* **412,** 561–565
46. Maurer-Stroh, S., Dickens, N. J., Hughes-Davies, L., Kouzarides, T., Eisenhaber, F., and Ponting, C. P. (2003) *Trends Biochem. Sci* **28,** 69–74
47. Huyen, Y., Zgheib, O., Ditullio, R. A., Jr., Gorgoulis, V. G., Zacharatos, P., Petty, T. J., Sheston, E. A., Mellert, H. S., Stavridi, E. S., and Halazonetis, T. D. (2004) *Nature* **432,** 406–411
48. Ahmed, S., Palermo, C., Wan, S., and Walworth, N. C. (2004) *Mol. Cell. Biol.* **24,** 3660–3669
49. Noh, B., Lee, S. H., Kim, H. J., Yi, G., Shin, E. A., Lee, M., Jung, K. J., Doyle, M. R., Amasino, R. M., and Noh, Y. S. (2004) *Plant Cell* **16,** 2601–2613
50. Sun, Y., Grimmler, M., Schwarzer, V., Schoenen, F., Fischer, U., and Wirth, B. (2005) *Hum. Mutat.* **25,** 64–71

Functional Characterization of JMJD2A, a Histone Deacetylase- and Retinoblastoma-binding Protein

Steven G. Gray, Antonio H. Iglesias, Fernando Lizcano, Raul Villanueva, Sandra Camelo, Hisaka Jingu, Bin T. Teh, Noriyuki Koibuchi, William W. Chin, Efi Kokkotou and Fernando Dangond

J. Biol. Chem. 2005, 280:28507-28518.
doi: 10.1074/jbc.M413687200 originally published online May 31, 2005
